

# Identification of old tidal dwarfs near early-type galaxies from deep imaging and H I observations

Pierre-Alain Duc,<sup>1\*</sup> Sanjaya Paudel,<sup>1</sup> Richard M. McDermid,<sup>2</sup> Jean-Charles Cuillandre,<sup>3</sup> Paolo Serra,<sup>4</sup> Frédéric Bournaud,<sup>1</sup> Michele Cappellari,<sup>5</sup> Eric Emsellem<sup>6,7</sup>

<sup>1</sup>Laboratoire AIM Paris-Saclay, CEA/IRFU/Sap, CNRS/INSU, Université Paris Diderot, 91191 Gif-sur-Yvette Cedex, France

<sup>2</sup>Gemini Observatory, Northern Operations Centre, 670 N. A'ohoku Place, Hilo, HI 96720, USA

<sup>3</sup>Canada-France-Hawaii Telescope Corporation, 65-1238 Mamalahoa Hwy., Kamuela, Hawaii 96743 USA

<sup>4</sup>CSIRO Astronomy and Space Science, Australia Telescope National Facility, PO Box 76, Epping, NSW 1710, Australia

<sup>5</sup>Sub-department of Astrophysics, Department of Physics, University of Oxford, Denys Wilkinson Building, Keble Road, Oxford OX1 3RH

<sup>6</sup>European Southern Observatory, Karl-Schwarzschild-Str. 2, 85748 Garching, Germany

<sup>7</sup>Centre de Recherche Astrophysique de Lyon, Université Lyon 1, Observatoire de Lyon, Ecole Normale Supérieure de Lyon, CNRS, UMR 5574, 9 avenue Charles André, F-69230 Saint-Genis Laval, France

Accepted for publication in MNRAS

## ABSTRACT

It has recently been proposed that the dwarf spheroidal galaxies located in the Local Group disks of satellites (DoSs) may be tidal dwarf galaxies (TDGs) born in a major merger at least 5 Gyr ago. Whether TDGs can live that long is still poorly constrained by observations. As part of deep optical and H I surveys with the CFHT MegaCam camera and Westerbork Synthesis Radio Telescope made within the ATLAS<sup>3D</sup> project, and follow-up spectroscopic observations with the Gemini-North telescope, we have discovered old TDG candidates around several early-type galaxies. At least one of them has an oxygen abundance close to solar, as expected for a tidal origin. This confirmed pre-enriched object is located within the gigantic, but very low surface brightness, tidal tail that emanates from the elliptical galaxy, NGC 5557. An age of 4 Gyr estimated from its SED fitting makes it the oldest securely identified TDG ever found so far. We investigated the structural and gaseous properties of the TDG and of a companion located in the same collisional debris, and thus most likely of tidal origin as well. Despite several Gyr of evolution close to their parent galaxies, they kept a large gas reservoir. Their central surface brightness is low and their effective radius much larger than that of typical dwarf galaxies of the same mass. This possibly provides us with criteria to identify tidal objects which can be more easily checked than the traditional ones requiring deep spectroscopic observations. In view of the above, we discuss the survival time of TDGs and question the tidal origin of the DoSs.

**Key words:** galaxies: abundances – galaxies: dwarf – galaxies: elliptical and lenticular, cD – galaxies: fundamental parameters – galaxies: interactions

## 1 INTRODUCTION

The discovery that a large fraction of Local Group (LG) dwarf galaxies are located within narrow planar structures, the so-called Disk of Satellites (DoSs), first speculated by Lynden-Bell (1976), and confirmed through a number of deep surveys, raised the question of their origin (Metz & Kroupa 2007; Ibata et al. 2013). Whether conventional  $\Lambda$ CDM cosmology can produce or not such DoSs is actively debated (Libeskind et al. 2011; Pawlowski et al. 2012; Bellazzini et al. 2013). Alternatively, the presence of DoSs might simply be accounted for if all dwarfs were formed simultane-

ously within a single parent structure, e.g. the collisional debris of a merger (Hammer et al. 2013). Objects born with that process are known as tidal dwarf galaxies (TDGs). The importance of TDGs among the dwarf population is rather controversial. On the one hand, the idealized numerical simulations of galaxy-galaxy collisions made by Bournaud & Duc (2006) suggest that only fine-tuned orbital parameters, mass ratio and initial gas content are needed for a merger to produce long-lived TDGs. Bournaud & Duc (2006) estimate that, at most, ten percent of dwarfs are of tidal origin. On the other hand, according to other numerical models (Dabringhausen & Kroupa 2013) and an extrapolation at high redshift of the TDG production rate (e.g. Okazaki & Taniguchi 2000), the majority of nearby dwarfs should be of tidal origin.

\* E-mail: paduc@cea.fr

The actual number of TDGs in the Universe is poorly constrained by observations. All TDGs so far unambiguously identified and studied in detail are found in on-going or very recent mergers: they are still linked to their parents by an umbilical cord – the tidal tail in which they were born –, are extremely gas-rich compared to other dwarfs and most likely have just become gravitationally bound (see review by [Duc 2012](#)). Among the TDG candidates identified so far with  $H\alpha$  or UV surveys (e.g. [Weilbacher et al. 2000](#); [Mendes de Oliveira et al. 2001](#); [Neff et al. 2005](#); [Hancock et al. 2009](#); [Smith et al. 2010](#); [Kaviraj et al. 2012](#); [Miralles-Caballero et al. 2012](#)), a large fraction are certainly gravitationally unbound star-forming knots that will quickly dissolve, or young compact star clusters that might evolve into globular clusters. In such conditions, estimates of the TDG fraction among regular galaxies substantially vary from one study to the other. This fraction may also depend on the large-scale environment. [Kaviraj et al. \(2012\)](#) estimated it to 6 % in clusters, [Sweet et al. \(2014\)](#) to 16 % in groups, whereas [Hunsberger et al. \(1996\)](#) claimed that it could be as high as 50 % in compact groups.

How TDGs evolve and for how long they survive is largely uncertain. Objects that are not kicked out from their parents are subject to dynamical friction, the gradual loss of orbital energy plunging them into the host system again, to destructive tidal forces generated by the deep gravitational potential of the host galaxies ([Mayer et al. 2001](#); [Fleck & Kuhn 2003](#)), or even to the destabilizing effect of ram pressure ([Smith et al. 2013](#)). The scenarios leading to a tidal origin for the MW and M31 satellites assume a very old merger (5–9 Gyr, [Hammer et al. 2013](#)). Can TDGs survive that long, and after several Gyr of evolution resemble present day Local Group dSphs, as proposed by [Dabringhausen & Kroupa \(2013\)](#)? Besides, the morphological and color evolution of TDGs will depend on their ability to continue forming stars, and thus to retain their original large gas reservoir. TDGs have a star-formation efficiency which is comparable to that of spiral galaxies ([Braine et al. 2001](#)). Thus, compared to regular dwarfs, their gas depletion time scale is rather large, and star-formation activity may in principle continue for a Hubble time. However, the quenching mechanisms that apply to regular satellites, such as ram pressure ([Mayer et al. 2006](#)) should also apply to TDGs and even be reinforced ([Smith et al. 2013](#)), presumably leading to a rapid reddening of their stellar populations.

The observation of several Gyr old TDGs is thus most needed to investigate the various scenarios proposed so far for the long-term evolution of such objects. Unfortunately when the tidal features in which they were born gradually evaporate – in typically 2 Gyr, according to numerical simulations ([Hibbard & Mihos 1995](#); [Michel-Dansac et al. 2010](#)) –, galaxies of tidal origin become more difficult to distinguish from classical ones. In principle, clear distinguishing criteria exist: a lack of dark matter<sup>1</sup>, and an unusually high metallicity for their mass (e.g. [Hunter et al. 2000](#); [Duc et al. 2007](#); [Sweet et al. 2014](#)). In practice, such characteristics need to be checked with high-resolution spectroscopic data, which are expensive in terms of telescope time. This is in particular the case for the low-surface-brightness dwarfs in which star-formation has already been quenched. The oldest TDGs disclosed so far based on their excess of metals and deficit of dark matter are located in the vicinity of advanced but still relatively recent mergers: e.g., NGC 7252 ([Belles et al. 2014](#)), or highly perturbed early-type galaxies, like

NGC 4694 in the Virgo Cluster ([Duc et al. 2007](#)). These TDGs may be 0.5-2 Gyr old.

In this paper we detail the properties of a sample of dwarf galaxies which are satellites of early-type galaxies (ETGs). They were initially found during a systematic deep imaging survey of ETGs with the Canada-France-Hawaii Telescope made as part of the ATLAS<sup>3D</sup> project ([Cappellari et al. 2011](#)). Their location towards faint streams of stars, visible on CFHT MegaCam images, or neutral hydrogen clouds, imaged by the Westerbork Synthesis Radio Telescope (WSRT, [Serra et al. 2012](#)), also as part of ATLAS<sup>3D</sup>, made them putative TDG candidates ([Duc et al. 2011](#)). Their association with fully relaxed galaxies, classified as lenticulars or ellipticals, rather than on-going mergers, ensured they are at least 2 Gyr old. The objects were followed up with the spectrograph GMOS installed on the Gemini-North telescope. The spectroscopic observations are presented in Section 2. Results on the metallicity and light profiles of the TDG candidates are given in Section 3. Finally, Section 4 discusses the implications of these observations on the long-term evolution of TDGs and proposes new diagnostics of a tidal origin that are based on scaling relations. They are applied to the Local Group dwarfs.

## 2 OBSERVATIONS

### 2.1 Sample

Fields around massive ETGs are the natural environment for the search of old TDGs as the latter form preferentially during major mergers. It is indeed difficult to extract the building material of TDGs in mergers involving galaxies with mass ratios below 1:5 ([Bournaud & Duc 2006](#)). The stellar body resulting from major merger events is most often an ETG-like object (e.g. [Bois et al. 2011](#)). So if long-lived TDGs exist, they should be present in environments which host at least one ETG. Note however that this condition does not necessarily apply to TDGs formed in the distant Universe. Collisions at redshift of 2 or above were presumably very different than nearby ones, involving galaxies with higher gas fraction, presumably containing massive clumps and being actively fed by external gas sources.

The host galaxies were selected from the ATLAS<sup>3D</sup> sample of nearby ( $D < 42$  Mpc) early-type galaxies ([Cappellari et al. 2011](#)), which benefit from a wealth of multi-wavelength data. Of relevance for this study are the extremely deep images obtained with the MegaCam camera installed on the CFHT ([Duc et al. 2011](#)) and the H I maps obtained with the WSRT ([Serra et al. 2012](#)). The selected ETGs exhibit in their vicinity low-surface brightness stellar and/or H I clouds, that might be collisional debris of past gas-rich major mergers. They are shown in Fig. 1. The targets for the spectroscopic follow-up, listed in Table 1, are within a distance of 200 kpc from the ETGs. Their radio velocity, less than  $600 \text{ km s}^{-1}$  with respect to the hosts, ensures that they are likely members of the ETG group. The targets were selected in part because of their association with gas clouds; they therefore likely contain star-forming regions and ionized gas, allowing us to measure the oxygen abundance from the nebular lines. Their surface brightness maps are shown in Fig. 1, together with the H I 21 cm contours.

Among the selected ETGs, NGC 5557 appears as the most promising system for hosting old TDGs. Indeed, as shown in [Duc et al. \(2011\)](#), the galaxy exhibits on MegaCam images several prominent features typical of merger remnants such as 200 kpc long stellar filaments, plumes and shells. Its eastern tidal tail hosts three

<sup>1</sup> The material forming TDGs emanate from the dark matter poor disk of spiral galaxies.

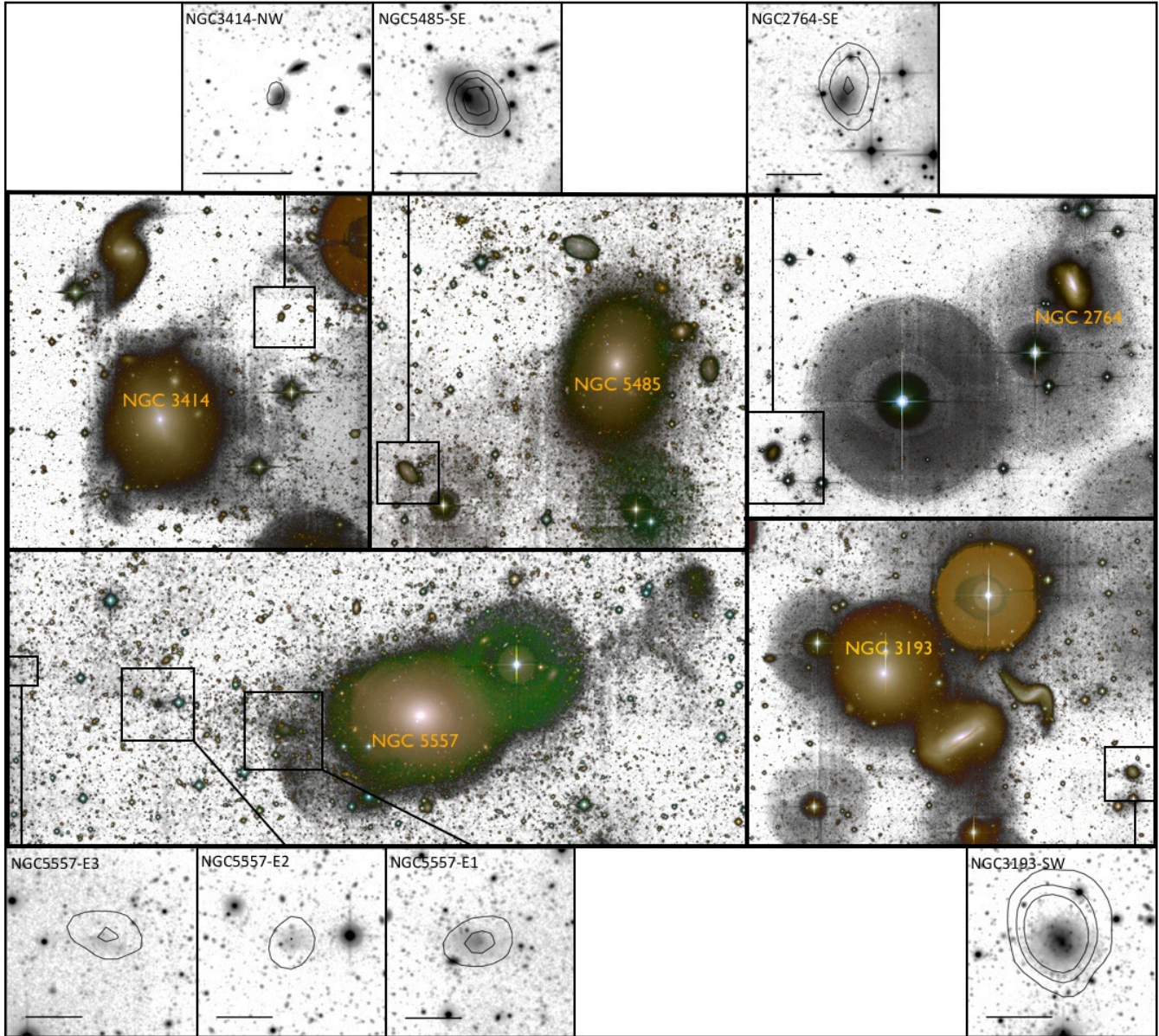


**Figure 1.** *Central panels:* composite  $g'+r'$  or  $g'+r'+i'$  MegaCam images of the early-type galaxies hosting the dwarf galaxies studied here. The faintest low surface brightness features are shown as inverted grey maps for better contrast. The ETG satellites for which a spectroscopic follow-up was carried out are indicated with the squares. *Top and bottom panels:* MegaCam  $g'$ -band surface brightness maps of the pre-selected satellites. The field of view of each panel is  $3 \times 3$  arcmin. Each bar corresponds to a physical length of 10 kpc. Greyscale levels range between 22 and  $28.5 \text{ mag.arcsec}^{-2}$ . H I contours from the WSRT observations are superimposed. Levels correspond to  $0.7, 1.4$  and  $2.1 \times 10^{20} \text{ cm}^{-2}$ .

blue objects, and associated with them, three isolated H I clouds, referred later as NGC 5557-E1, E2 and E3.

Note that the sample is by no means complete. A systematic investigation of the origin of ETG satellites is beyond the scope of this pilot study.

## 2.2 Observations

Spectroscopic observations of the TDG candidates were carried out between March and June 2012 using Gemini Multi-Object Spectrograph (GMOS) on the 8.1 meter Gemini-North telescope (as part of program GN-2012A-Q-103). The B600\_G5307 grating was used together with a long slit. Its width was 1.3 arcsec, leading to an in-

strumental resolution of  $4 \text{ \AA}$  FWHM. We used two slightly different grating tilts for each galaxy in order to fill the gap between the camera chips. The final wavelength coverage was  $4100 \text{ \AA} - 6900 \text{ \AA}$ . One single slit, positioned parallel to the major photometric axis, was used for all targets, except for NGC 5557-E1 which benefited from observations along two directions, as shown in Figure 2. Total exposure times ranged between 0.5 hour for the most luminous dwarfs to 1.7 hour for the faintest ones, in particular those around NGC 5557.

Spectrophotometric calibration was performed using a single observation of the baseline standard star (G191-B2B) taken separately from the science data, but with a matching instrument configuration.

**Table 1.** Location of the ETG satellites

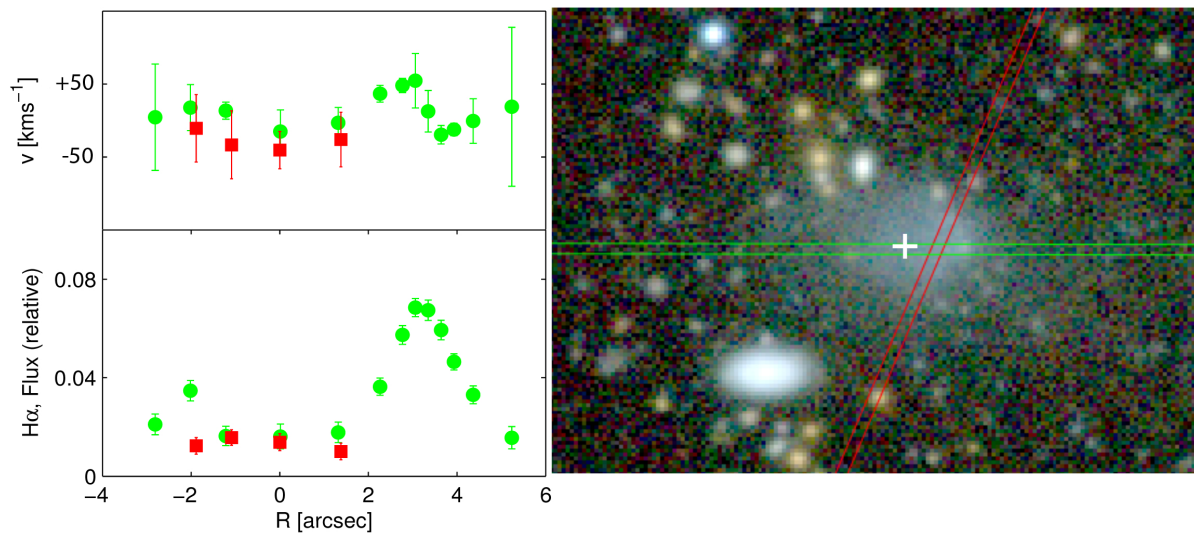
Galaxy	RA J2000 (1)	Dec J2000 (2)	D Mpc (3)	V(H I) km s <sup>-1</sup> (4)	V(opt) km s <sup>-1</sup> (5)	V(H I)-V(host) km s <sup>-1</sup> (6)
NGC2764-SE	9:08:55.8	21:21:37	39.6	2680	2714 ± 12	-26
NGC3193-SW	10:17:23.3	21:47:58	33.1	1940	1964 ± 12	559
NGC3414-NW	10:50:49.5	28:03:30	24.5	1535	1437 ± 40	65
NGC5485-SE	14:08:26.8	54:54:32	25.2	1408	1389 ± 12	-519
NGC5557-E1	14:18:55.9	36:28:57	38.8	3252	3308 ± 40	33
NGC5557-E2	14:19:24.5	36:30:05	38.8	3196	–	-23
NGC5557-E3	14:19:58.1	36:31:53	38.8	3165	–	-54

Notes: (3) Assumed distance (4) H I heliocentric velocity determined from the WSRT moment 1 maps (5) Optical heliocentric velocity determined from GMOS (6) Difference between the velocity of the satellite and that of the central ETG

**Table 2.** Structural and chemical properties of the ETG satellites

Galaxy	$M_V$ mag (1)	$M_*$ 10 <sup>8</sup> M <sub>⊙</sub> (2)	$R_e$ kpc (3)	$\mu_{g0}$ mag arcsec <sup>-2</sup> (4)	$n$ dex (5)	12+log(O/H) (6)
NGC 2764-SE	-16.3 ± 0.05	3.9 ± 1.5	1.4 ± 0.05	22.8 ± 0.1	0.7	8.3
NGC 3193-SW	-16.8 ± 0.05	5.6 ± 2.2	1.3 ± 0.05	22.1 ± 0.1	1.0	8.3
NGC 3414-NW	-14.3 ± 0.05	0.4 ± 0.1	0.8 ± 0.05	22.8 ± 0.1	0.7	8.2
NGC 5485-SE	-17.0 ± 0.05	11.0 ± 3.3	1.7 ± 0.05	21.7 ± 0.1	1.3	8.4
NGC 5557-E1	-14.7 ± 0.1	1.2 ± 0.7 (1.4)	2.3 ± 0.1	24.3 ± 0.2	1.3	8.6
NGC 5557-E2	-13.0 ± 0.1	0.15 ± 0.1	1.8 ± 0.7	26.1 ± 0.2	0.6	–

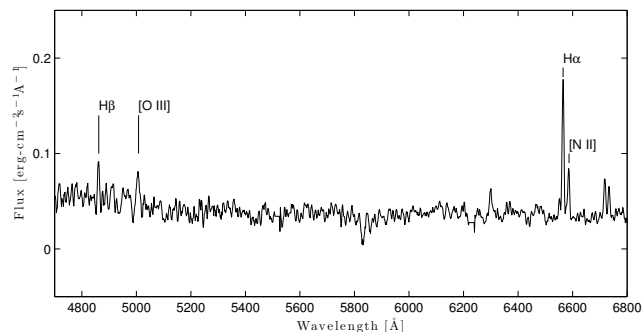
Notes: (1) Absolute magnitude in the V band determined from the MegaCam images, corrected for galactic extinction. The g' to V band conversion was done with the formula given in the SDSS DR7 on-line documentation (Lupton, 2005) (2) Stellar mass estimated from the MegaCam g' band flux and g' - r' color, using the prescriptions of Bell et al. (2003). For NGC 5557-E1, the stellar mass determined from the integrated star formation history is given in parentheses (3) Effective radius measured from the light profile fitting in the g'-band (4) Extrapolated central surface brightness in the g'-band (5) Sérsic index determined for the light profile fitting (6) Oxygen abundance estimated from the N2 method, and the calibration of Marino et al. (2013)



**Figure 2.** Gas kinematic profiles of NGC 5557-E1 as extracted from the two long slits. Their directions, shown superimposed on the true color image of the dwarf to the right (composite g'+r'+i'), roughly correspond to the major and minor axis. The colors of the data points and slits match. Position 0 on the kinematics profile indicates where the two slits intercept. The morphological center of the dwarf, as determined from the light profile fitting, is indicated with a plus sign.

**Table 3.** Spectrophotometry of NGC 5557-E1

$H\beta$	$100 \pm 18$
$[\text{OIII}]_{\lambda 5007}$	$92 \pm 18$
$[\text{NII}]_{\lambda 6548}$	$48 \pm 8$
$H\alpha$	$307 \pm 12$
$[\text{NII}]_{\lambda 6584}$	$124 \pm 8$
$[\text{SII}]_{\lambda 6717}$	$109 \pm 4$
$[\text{SII}]_{\lambda 6731}$	$82 \pm 6$
Extinction coefficient at $H\alpha$	$0.2 \pm 0.1$
$H\alpha$ flux	$6.4 \pm 0.1 \times 10^{-15} \text{ erg s}^{-1} \text{ cm}^{-2}$
$\text{SFR}(H\alpha)$	$7.2 \pm 0.1 \times 10^{-3} M_{\odot} \text{ yr}^{-1}$


**Figure 3.** GMOS optical spectrum of the spectroscopically confirmed TDG NGC 5557-E1.

The GMOS spectra were reduced using the *gmoss* Gemini package within IRAF. Basic data reduction includes bias subtraction, cosmic ray removal, flat field correction, wavelength calibration, and flux calibration. Because some of our targets had a surface brightness much lower than the sky brightness, special care was taken with the sky background subtraction. One dimensional spectra were then extracted after rectification of the 2D frame and summing up along the slit in the region showing  $H\alpha$  emission. Figure 3 displays the one-dimensional spectra of NGC 5557-E1, extracted and recombined from the two 2D frames acquired for this object. The emission-line fluxes were measured from the flux calibrated spectra using the IRAF task *splot*. Spectrophotometric data for NGC 5557-E1, our confirmed TDG as argued later, are listed in Table 3. We did not find signatures of absorption lines in the extracted spectra, and thus did not correct the Balmer lines for any underlying absorption features. The extinction coefficient was determined from the Balmer decrement assuming a theoretical value of the  $H\alpha/H\beta$  flux ratio of 2.86 and applied to the emission line fluxes using the Calzetti et al. (2000) extinction law.

The photometric data used in this paper have been measured on CFHT / MegaCam images acquired as part of the ATLAS<sup>3D</sup> survey. They are presented in Duc et al. (2011) and Duc et al. (2014, in prep.). Images in the  $g'$  and  $r'$  bands are available for all our targets. NGC 5557 was also observed in the  $i'$  band.

### 3 RESULTS

We determined the spectrophotometric properties of all our targets, with the aim of confirming the physical association of the dwarfs with the host galaxy, and testing their tidal origin using a deviant gas-phase metallicity as a primary criterion.

#### 3.1 Velocities and physical association

We derived the radial velocity of all observed dwarf galaxies by taking the mean redshift of all detected emission lines. The calculated uncertainties are the standard deviation of the measured radial line velocities. The optical velocities of the targets are listed in Table 1 together with the H I velocities. The difference between the optical and radio velocities ranges between 20 and  $100 \text{ km s}^{-1}$  confirming the physical association between the stars and the gas for all ETG satellites. The absence of emission lines in NGC 5557-E2 and NGC 5557-E3 (despite the presence of H I gas) did not allow us to determine their optical redshift. Furthermore due to the low surface brightness of these galaxies, no stellar continuum could be extracted. Note however that the H I velocities of E2 and E3 also match that of E1, suggesting that they all belong to the same structure (Duc et al. 2011).

#### 3.2 Spectrophotometric properties

A physical determination of the gas-phase metallicity requires knowing the electron temperature, usually estimated measuring the  $[\text{OIII}]_{\lambda 4363}$  emission line. Unfortunately, this emission line is extremely weak and not detectable in the faint dwarf galaxies studied here. We have instead estimated the oxygen abundance using the so-called  $N2$  empirical method, which makes use of the strong  $H\alpha$  and  $[\text{NII}]$  line fluxes. The method, although indirect – it assumes a standard N/O abundance ratio – relies on the flux ratio between two lines with close wavelengths and thus has the main advantage of being little affected by uncertainties in the flux calibration or dust extinction. Systematics errors of the method are about 0.2 dex. The oxygen abundances determined with the recent calibration of  $N2$  by Marino et al. (2013) are listed in Table 2.

Our estimated oxygen abundances are plotted in Fig. 4 against the absolute V-band magnitude. On this figure, we added for reference samples of young tidal dwarf galaxies from the literature (Weilbacher et al. 2003; Duc et al. 2007), of nearby star-forming dwarf irregular galaxies from Richer & McCall (1995) and van Zee & Hayes (2006), as well as dwarf galaxies queried from the SDSS archives having  $g-r < 0.4 \text{ mag}$ , a redshift range between 0.007 and 0.015, and oxygen abundances derived by ourselves with the same  $N2$  method. Whereas pristine dwarfs globally follow, though with some scatter, a luminosity/mass-metallicity relation, TDGs do not and have a too high metallicity for their luminosity. This reflects their very origin – they are made of pre-enriched material – and is a strong criterion to identify recycled objects. On this relation, the dwarfs studied here lie between the locus of normal dwarfs and those of TDGs, leaving open the possibility that some of them may in fact be of tidal origin. One object suffers no ambiguity: NGC 5557-E1. With an oxygen abundance of  $12+\log(\text{O}/\text{H})=8.6$ , i.e. close to solar (Asplund et al. 2005)<sup>2</sup>, the dwarf deviates by 0.6 dex from the standard luminosity-metallicity relation: the difference is much higher than the scatter of the relation and systematic uncertainties in the metallicity measurement of about 0.2 dex.

<sup>2</sup> The empirical method based on the combination of  $[\text{OIII}]_{\lambda 5007}$  and  $[\text{NII}]_{\lambda 6584}$  line – the so called O3N2 method, as calibrated by Marino et al. (2013) –, would give an abundance close to that obtained with  $N2$ :  $12+\log(\text{O}/\text{H})=8.5$ , but with a larger measurement uncertainty due to the faintness of the  $[\text{OIII}]_{\lambda 5007}$  line flux (see Fig. 3).

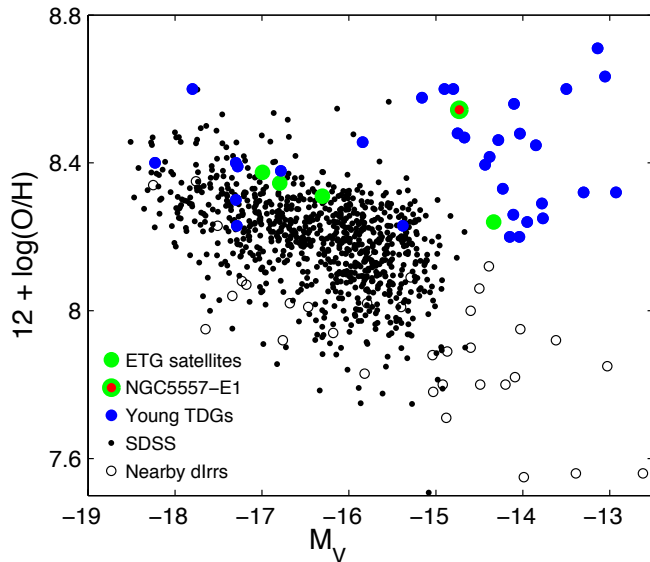


**Figure 4.** Gas phase oxygen abundance versus absolute magnitude for various samples of star-forming dwarf galaxies. The open circles are nearby dwarf irregular galaxies (Richer & McCall 1995; van Zee & Haynes 2006); the small black dots are SDSS dwarf galaxies (see main text for details). The larger green dots are the ETG satellites studied here, with the spectroscopically confirmed old TDG pointed with the central red dot. Young TDGs from the literature are displayed with the blue dots (Weilbacher et al. 2003; Boquien et al. 2010). Note that the oxygen abundances of the SDSS dwarfs and ETG satellites have been determined with the same  $N_2$  method and calibration. Those for the other dwarfs, compiled from the literature, were estimated using various methods.

### 3.3 Photometric properties

The data reduction of the ultra-deep MegaCam images and quality control are presented in Duc et al. (2011). The stellar masses of the dwarf satellites were estimated from the MegaCam  $g'$  band flux and  $g' - r'$  color, using the stellar mass to light ratios given in Bell et al. (2003).

We used the IRAF *ellipse* task to derive the  $g'$ -band light profile of the dwarfs. Before performing the ellipse fitting, we subtracted the faintest point-like sources from the images, replacing them with the surrounding sky and masked the background and foreground larger and brighter objects. In the case of NGC 5557-E1, which, at the depth of our images, is located within the extended stellar halo of its host galaxy, a model of the host was first subtracted from the image to minimize the contamination. The ellipse fitting of the dwarf was initially performed fixing the centre of the galaxy while allowing a variation of the ellipticity and position angle (PA). To obtain the surface photometric parameters, a final run of *ellipse* was done, this time fixing the PA at a value corresponding to the average of the PAs at the outer isophotes.

As examples, the light profiles of NGC 5557-E1 and NGC 5557-E2 are shown in Fig. 5. They are well fitted by close-to-exponential Sérsic profiles (Sérsic 1968), with an index  $n$  of resp. 1.3 and 0.6. Due to its extremely low surface brightness and disturbed morphology, the light profile of NGC 5557-E3 could not be properly determined. The derived effective radii,  $R_e$ , and central surface brightnesses of all the dwarfs in our sample are listed in Table 2, and plotted against their stellar mass in Figs 6 and 7, together with various samples of nearby dwarf galaxies, either star-forming or passive, taken from the literature. We also added a sample of

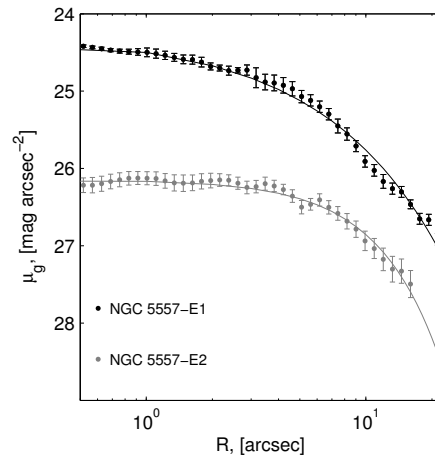


**Figure 5.**  $g'$ -band surface brightness profiles along the major axis of the two confirmed old TDGs in our sample. Sérsic profiles are superimposed. Parameters are given in Table 2.

young TDGs, for which we have measured the effective radius with the same method (see details on the data and measurements in Table 4). The uncertainties listed in Table 2 correspond to the errors in the photometric measurements (absolute magnitude, stellar masses), and galaxy profile modeling (effective radius). With an effective radius as large as resp. 2.3 and 1.8 kpc, NGC 5557-E1/E2 occupy, like the young TDGs, the upper locus of the size-mass relation. Besides, the two dwarfs also stand out in the central surface brightness versus stellar mass relation, lying on the low-surface-brightness edge of the relation.

### 3.4 Detailed properties of NGC 5557-E1

On all the diagrams discussed above: metallicity, effective radius and central surface brightness versus luminosity/mass, NGC 5557-E1 is located at the edge of the distributions with respect to reference classical dwarfs, or even appears as an outlier. In particular, as further argued in Sect. 4.1, its high relative metallicity with respect to its luminosity leaves little doubts it is a TDG. In the following we focus our analysis on this specific object, and present further details on its internal properties.

#### 3.4.1 Stellar populations

On the MegaCam composite  $g' + r' + i'$  image (see Fig. 2, right), and  $g' - r'$  color profile (see Fig. 8), NGC 5557-E1 appears as a rather blue object, suggesting recent or ongoing star formation activity. Indeed, the galaxy has a significant H I gas reservoir: its gas fraction, H I to visible mass, is above 50%. Its detection in two UV-bands (FUV and NUV of GALEX) indicates ongoing star formation activity at a rather low level:  $5 \times 10^{-3} M_{\odot} \text{ yr}^{-1}$  (Duc et al. 2011).

Our long-slit spectroscopic spectra indicate the presence of ionized gas over a range of 5 arcsec – about 1 kpc at the distance of the galaxy – (see Fig. 2), confirming the presence of extended regions of star formation. The H II regions are however offset with respect to the morphological center. We have obtained another estimate of the SFR from the integrated  $H_{\alpha}$  luminosity, corrected from dust extinction (see Table 3). The aperture correction was performed by extrapolating the  $H_{\alpha}$  line measured within the long slits out to the entire galaxy. The SFR was then determined using the

**Table 4.** Stellar properties and surface brightness parameters of a sample of young TDGs

Galaxy	$M_V$ mag	$M_*$ $10^7 M_\odot$	$R_e$ kpc	$\mu_0$ mag arcsec $^{-2}$	$n$	Ref
	(1)	(2)	(3)	(4)	(5)	(6)
ARP 105S	-16.9	6.6	5.7	20.1	1.7	NTT/EMMI ,a, c
NGC 7252E	-14.6	8.5	2.2	24.2	0.8	ESO2.2m/WFC, d
NGC 7252N	-14.7	9.4	2.6	22.1	2.7	ESO2.2m/WFC, c, d
VCC 2062	-13.2	4.7	2.4	24.7	1.0	CFHT/MegaCam, b, c

Notes: (1) Absolute magnitude in the V band (2) Total stellar mass derived from SED fitting (3) Effective radius measured from the light profile fitting (4) Extrapolated central surface brightness in the V band (5) Sérsic index used for the light profile fitting (6) Reference images used for the surface brightness analysis (this paper) and bibliography: a: [Duc & Mirabel \(1994\)](#), b: [Duc et al. \(2007\)](#), c: [Boquien et al. \(2010\)](#), d: [Belles et al. \(2014\)](#)

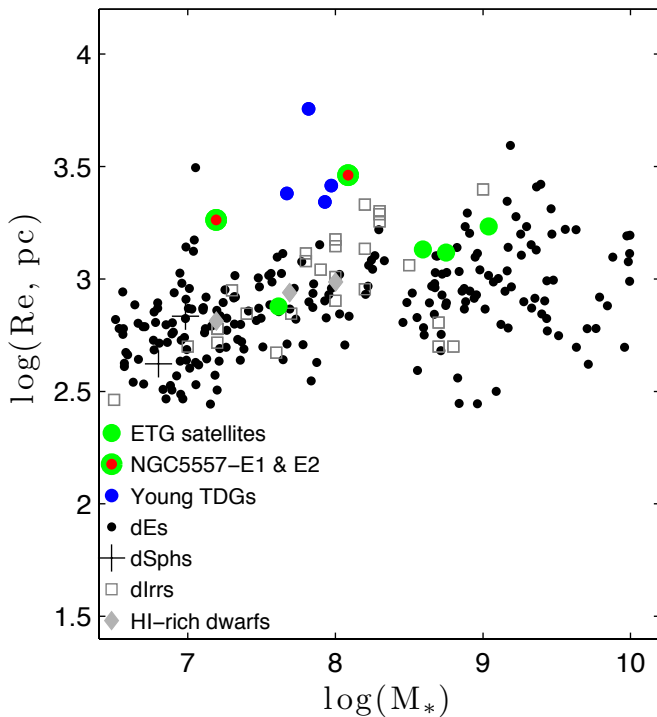


**Figure 6.** Effective radius versus stellar mass for various samples of dwarf galaxies. The small black points resp. crosses correspond to the compilation of dEs resp. dSphs made by [Mizgale & Hilker \(2011\)](#). The grey open squares are nearby dwarf irregular galaxies extracted from the sample of [Kirby et al. \(2008\)](#), and the grey diamonds are H I-selected star-forming dwarfs from [Duc et al. \(1999\)](#). The larger green dots are the ETG satellites studied here, with the confirmed old TDGs pointed with the central red dots. Total stellar masses were estimated from the MegaCam  $g'$  and  $r'$  bands, using the prescriptions of [Bell et al. \(2003\)](#). Young TDGs from the literature are displayed with the blue dots.

calibration given by [Kennicutt \(1998\)](#). The derived SFR is within 25 % of that determined from the UV, confirming its rather low value.

Fitting our multi-wavelength data points ( $FUV, NUV, g', r', i'$ ; see values in Table 3 of [Duc et al. 2011](#)) with the stellar population models of [Bruzual & Charlot \(2003\)](#), we made an attempt to reconstruct the star formation history of the galaxy. We constrained the model with a fixed metallicity of about solar, consistent with the measured one,

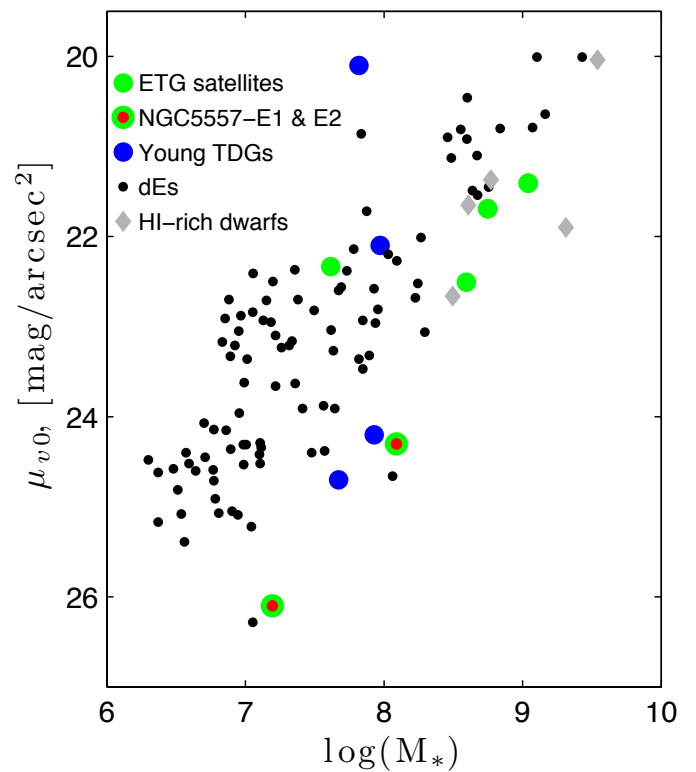


**Figure 7.** Extrapolated central surface brightness in the V band versus stellar mass for various samples of dwarf galaxies. The black dots correspond to the sample of early-type dwarfs from [Mizgale et al. \(2008\)](#). The grey diamonds are star-forming H I-selected star-forming dwarfs from [Duc et al. \(1999\)](#). The larger green dots are the ETG satellites studied here, with the confirmed old TDGs pointed with the central red dots. Young TDGs from the literature are displayed with the blue dots.

varied the extinction,  $A_V$ , between 0.1 and 0.3 mag, within the observed range. We further assumed an exponentially declining star-formation history after an initial burst of star formation, with a  $\tau$  value of 0.9 Gyr. The best fit<sup>3</sup>, shown in Fig. 9, is obtained with an initial burst 4 Gyr ago, and an extinction of 0.3 mag. The model predicts an instantaneous current star-formation rate of  $11 \times 10^{-3} M_\odot \text{ yr}^{-1}$ , within a factor of 2 that estimated from the  $H_\alpha$  and UV.

<sup>3</sup> which however under-predicts the NUV data point

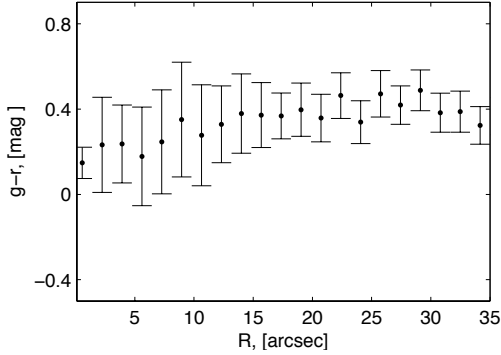


**Figure 8.**  $g'-r'$  color profile of NGC 5557-E1

The stellar mass derived from the integrated star formation history is  $1.4 \times 10^8 M_{\odot}$ , a value very close to that obtained from the  $g'$  band magnitude and color,  $1.2 \times 10^8 M_{\odot}$ . As argued in Section 4.1, this basic model gives a hint on the formation time of the object consistent with a tidal origin.

### 3.4.2 Kinematics

The kinematical profile of NGC 5557-E1 was derived from our long-slit spectroscopic data, fitting a Gaussian to the available emission lines, mainly  $H_{\alpha}$  and [NII]. Depending on the emission line flux strength, we averaged the spectrum by 3-5 pixels in the spatial direction to increase the signal-to-noise ratio. For each position along the slits, an estimate of the mean velocity and error was determined averaging the velocity from the different emission lines. With the grating used and seeing at time of observations, the uncertainties are estimated as approximately  $\pm 30 \text{ km s}^{-1}$ . The derived velocity profiles in two directions are shown in Fig. 2, together with the slit positions. The observed projected velocity gradients are about  $70 \text{ km s}^{-1}$  along the major axis and about  $20 \text{ km s}^{-1}$  along the minor one. Note that this is a crude method to determine the internal kinematics of a galaxy. First it may in principle be affected by slit effects<sup>4</sup>. Besides, as shown in Fig. 2, the kinematical and morphological centers do not seem to coincide. The evidence for rotation in this galaxy, if any, should be confirmed by integral field spectroscopic observations or sensitive high-resolution H I observations.

## 4 DISCUSSION

### 4.1 The dwarfs around NGC 5557: the oldest TDGs so far identified in the nearby Universe

Among the satellites of the early-type galaxies studied in this paper, one object stands out: NGC 5557-E1. With an oxygen abundance of about solar, in excess by about 0.6 dex with respect to the metallicity–luminosity relation, it is undoubtedly made of pre-enriched material. Such an oxygen abundance is typical of galaxies of stellar mass of about  $2 \times 10^9 M_{\odot}$  (see Fig. 4 and Tremonti et al. 2004), i.e. about 10 times more massive than NGC 5557-E1.

<sup>4</sup> In this particular case, the  $H_{\alpha}$  emission seems rather diffuse, limiting the slit effect, i.e. the artificial velocity gradients induced by the unknown position of the emission line regions within the slit width. The fact that the velocities at the location where the two slits intercept are within  $20 \text{ km s}^{-1}$  of each other is a further indication that there is no major slit effect.

The MegaCam images revealed that NGC 5557-E1 is located within a giant stellar stream. The total stellar mass in these collisional debris is estimated to about 2–4% that of NGC 5557 (Duc et al. 2011), i.e. about  $5 \times 10^9 M_{\odot}$ . Thus in principle there is enough material in the tails to contain the debris of a pre-existing satellite that would have lost 90% of its initial mass. However, as seen in Fig. 1, these debris are distributed over large distances (370 kpc), are at some locations very broad and at others have shell like structures. This makes extremely unlikely the hypothesis that they all originate in a minor merger involving a  $2 \times 10^9 M_{\odot}$  satellite, and that NGC 5557-E1 is just its nucleus. Furthermore, such a scenario would predict a red remnant, and an S-shape for the tidal tails on each side of the object. This is not observed. NGC 5557-E1 is a diffuse, blue object, located within a long, straight tail which includes other gas condensations.

In such conditions, we can exclude that NGC 5557-E1 is the remnant of a disrupted, pre-existing satellite. This makes it a genuine tidal dwarf galaxy. We could not estimate the metallicity of its companion galaxy, NGC 5557-E2, because of its very low surface brightness and lack of ionized gas. However, given its location, further out along the same tidal tail, its H I velocity close to that of E1, it has most likely the same tidal origin. This might also be the case for NGC 5557-E3, located at the apparent tip of the tidal tail; however, its very perturbed, elongated morphology raise doubts on whether this condensation is gravitationally bound – another characteristic to warrant a TDG status. Thus, in the following for simplicity, we will call E1 and E2 confirmed old TDG candidates, although only the metallicity of E1 could be derived.

The lack of dark matter is certainly the most robust criterion to identify tidal dwarfs; it is also however the most difficult to check. In the case of NGC 5557-E1, a velocity curve in the ionized gas could be measured, with some evidence of a small gradient, perhaps indicating some rotation and that the galaxy is gravitationally bound. On the H I WSRT map, a small velocity gradient of about  $\sim 30 \text{ km s}^{-1}$  is observed along the dwarf (see Fig. 12 in Duc et al. 2011). Whether it traces the kinematics of the object or global streaming motions along the tail is however unclear. Our data clearly do not have the requested velocity resolution and spatial sampling to derive the dynamical mass and estimate the dark matter fraction. IFU spectroscopic data would be required for that.

How old are NGC 5557-E1/E2? The inner region of their host galaxy, NGC 5557, is fully relaxed. It does not contain any specific kinematical features (Krajnović et al. 2011) – the galaxy is a slow rotator – dust lanes, H I or CO clouds, or even young stellar populations that would indicate a recent major gas-rich merger. As shown among others by Di Matteo et al. (2008), merger driven starbursts are short lived with a duration activity of a few 100 Myr. The loss of memory of a merger event inside NGC 5557 allows us to estimate a minimum age for its TDGs of at least a couple of Gyr (Duc et al. 2011). On the other hand, the prominent tidal tails formed during the merger event are still visible on the ultra-deep images, though their average surface brightness is very low: around  $28.5 \text{ mag arcsec}^{-2}$ . They furthermore still contain gas clouds. Given the relative fragility of these structures and their fading with time, they should have formed at a redshift well below 1. The SED fitting of NGC 5557-E1 indicates that the galaxy contains a significant fraction of stars older than a couple of Gyr. The inferred star-formation history is consistent with an initial burst occurring 4 Gyr ago, which coincides with the dynamical time scale of its parent galaxy. If these age estimates are correct, NGC 5557-E1, and likely its companion E2, are the oldest confirmed TDGs so far discovered in the nearby Universe.



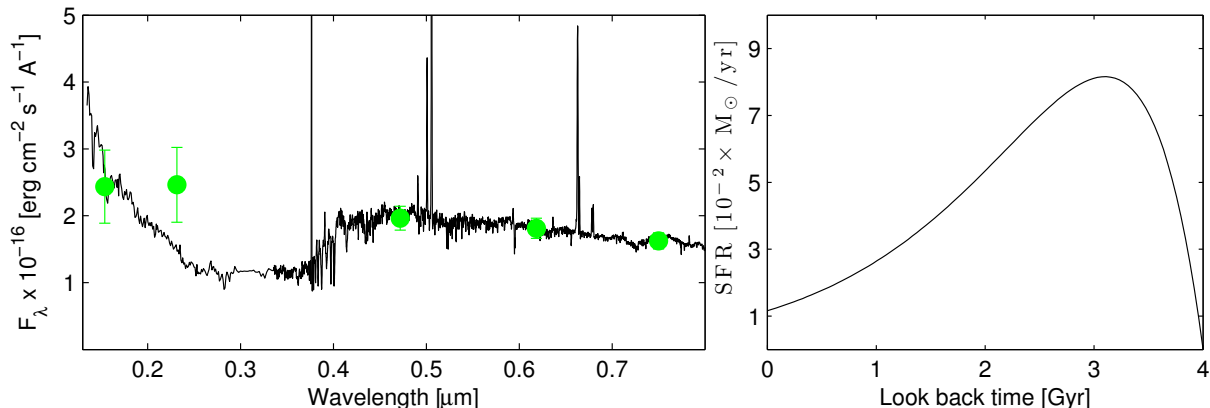


**Figure 9.** Spectral Energy Distribution of NGC 5551-E1. An evolutionary stellar synthesis model from Bruzual & Charlot (2003) is superimposed. The best fit is obtained with an exponentially declining starburst of age 4 Gyr. The corresponding star formation history is displayed to the right.

Simulations of galaxy mergers had predicted that under specific conditions massive tidal objects could form and survive for a few Gyr (Bournaud & Duc 2006). Our observations prove that this is indeed the case.

#### 4.2 The morphological and stellar evolution of tidal dwarf galaxies

NGC 5557-E1/E2 may be used as a laboratory and give hints on how TDGs look like after several Gyr of evolution. Previous idealized simulations of TDG-like objects, i.e. without dark matter, had made predictions on their morphological (Metz & Kroupa 2007; Dabringhausen & Kroupa 2013) and chemical evolution (Recchi et al. 2007). They concluded that evolved TDGs might resemble present-day dwarf ellipticals/spheroidals (dEs/dSphs). Such simulations were however so far weakly constrained by observations.

Like typical dwarf spheroidals, the light profile of NGC 5557-E1/E2 is indeed exponential. The surface brightness profile appears smooth, without showing prominent star-forming clumps, contrary to younger star-forming TDGs located at similar distances. The true color image of NGC 5557-E1 (see Fig. 2) and  $g' - i'$  color profile (see Fig. 8) show a rather homogenous stellar distribution with perhaps a weak reddening in the outskirts where its stars mix with that of the host tidal tail. However, the main distinguished features of E1/E2 are – besides the relatively high metallicity (for E1)– a low central surface brightness and large effective radius, compared to other dwarf galaxies of similar luminosity/mass and even gas content. As shown in Fig. 6, young TDGs observed in recent mergers already have an initially large  $Re$ . This seems preserved when TDGs become older, indicating that either tidal dwarfs do not manage to further condense due to internal feedback and/or are subject to some tidal stripping in their orbit around their host. Dabringhausen & Kroupa (2013) argue that the lack of dark matter in TDGs could explain their deviation from the mass-size relation. Stellar and gas mass loss contribute to change the internal dynamics of the galaxy and consequently its stellar distribution: the potential well of the system becomes shallower leading to an increase of the size.

In that respect it is worth noting that NGC 5557-E1/E2 kept a significant fraction of their gas reservoir. For instance, after a few Gyr of evolution, E1 only converted half of its H I gas reservoir into stars<sup>5</sup>. With a current SFR of  $5\text{--}10 \times 10^{-3} M_{\odot} \text{ yr}^{-1}$ , the galaxy

might continue to form stars at this rate for more than 10 Gyr. This is at odds with the observations of classical dSphs which lost all of their gas. As a matter of fact, it is puzzling to observe that the H I reservoir managed to remain bound to the stellar component of the old TDGs (see Fig. 1), despite internal feedback, tidal thrashing and even more ram pressure. The simulations of Smith et al. (2013) predict that dark matter poor galaxies subject to a wind for several Gyr should experience a strong decoupling between the gaseous and stellar components. This may indicate that the density of the hot gas surrounding the parent galaxy, or the relative velocities of the TDGs with respect to this gas, may not be as high as those assumed in the simulations. Recently, Ploeckinger et al. (2014) developed chemodynamical models showing the inefficiency of internal feedback and external stripping in removing the gas of TDGs.

#### 4.3 The identification of old TDGs: adding an extended radius as an additional criterion?

The spectrophotometric methods traditionally used to identify TDGs require prohibitive amounts of telescope time even for nearby objects. Indeed, the metallicity of TDGs – typically half solar to solar, which is independent of their mass/luminosity – become deviant only for objects with absolute V band magnitude fainter than  $-15$  (see Fig. 4). This is unfortunately the regime for which large-scale surveys such as the SDSS lack spectroscopic data. Furthermore, the chemical method does not apply when investigating a tidal origin for dwarfs that would have been formed in the early Universe when the metallicity of the parent galaxies was as low as today's dwarf galaxies.

A remarkable result from our study is that the two confirmed TDGs have a large effective radius (above 1.8 kpc) for their mass, a characteristic also observed in young starbursting TDGs. Assuming that NGC 5557-E1/E2 are representative of the TDG population, this property may provide a very practical way to identify among dwarf satellites those of tidal origin, even without spectroscopy. Instead optical images and light profile analysis might be good enough to at least pre-select TDG candidates formed long ago.

Obviously, this criterion is not unambiguous. Indeed, at least

ble, in agreement with simulations that indicate that TDGs are made from gas collapse and not instabilities in the stellar component (Duc et al. 2004; Wetzstein et al. 2007)

<sup>5</sup> For this estimate, we assumed that the initial stellar content was negligi-

a temporary size expansion is also expected for tidally threshed pre-existing dwarf galaxies, as illustrated in Paudel et al. (2013). However, deep images can be obtained to disclose possibly associated tidal tails. As argued above, their shape – linear or S-like– can then favor one hypothesis or the other. Besides, the very long term evolution of TDGs over a Hubble time has not been probed in our study. It is relevant to note that our confirmed TDGs have a very low rate of star-formation, the morphological appearance of dwarf spheroidals (except their large effective radius) but still contain gas, unlike typical fully passive dwarf satellites. However, the processes that will later trigger the star-formation quenching and stellar/gas mass loss should rather lead to an increase rather than a shrinking of the TDG size, unless bars develop in the satellites leading to a possibly temporary concentration of the stellar component (Mayer et al. 2001). Besides, mergers are able to produce much more compact objects, which may result in the formation of ultra-compact dwarf galaxies (Fellhauer & Kroupa 2002; Bournaud et al. 2008). Such objects which may also be long lived were not investigated in this paper.

In the survey presented in this paper, besides the dwarfs around NGC 5557, 4 other satellites had been selected for a spectroscopic follow-up. Three of them occupy the lower envelope of the mass-central surface brightness relation (Fig. 7) and the upper envelopes of the mass-effective radius (Fig. 6) and luminosity-metallicity (Fig. 4) relations. Thus, they are located towards regions where TDGs are expected to be found. On these diagrams, a few other objects selected from the SDSS seem to also have larger than expected effective radii and metallicities. But none of them, including our pre-selected satellites, deviate from these scaling relations the way the dwarfs around NGC 5557 do. To prove a tidal origin, further investigations should thus be carried out. Extremely deep imaging that are able to disclose very faint low-surface brightness tidal tails linking the satellites to their parents, such as the Next Generation Virgo Cluster Survey (NGVS, Ferrarese et al. 2012), or the on-going CFHT Large Programme MATLAS (Duc et al., 2014, in prep.), might help. In the survey presented here, such direct signatures were only found for the NGC 5557 dwarfs.

The large effective radius of old TDGs (for their mass) is consistent with a low central surface brightness. This low surface brightness means that the census of old TDGs from imaging surveys with limited surface brightness sensitivity, such as the SDSS, may miss most of the old TDG population. In fact NGC 5557-E1, E2 and E3 are barely visible on the Sloan images, as shown in Fig. 10.

#### 4.4 Implications for the origin of Local Group dwarfs

Until deep imaging/spectroscopic surveys are carried out, the Local Group remains the most convenient laboratory to investigate the fraction of tidal objects among old dwarfs. If some of the LG dSphs are of tidal origin, they should have been produced a long time ago, as the LG does not contain any vestige of a recent major merger. The metallicity method, and, more generally, criteria relying on the chemistry or stellar properties thus do not directly apply to these objects. However, as argued earlier, a relatively large effective radius might be a durable characteristic of a tidal origin.

In that respect, the dwarfs located within the disks of satellites, that were claimed as being old TDGs, are not located in specific regions of the scaling relations: only 10% of the M31 dSphs have effective radii larger than 1 kpc and none for the MW dSphs (Brasseur et al. 2011). This may weaken the TDG hypothesis, which was al-

ready challenged by the evidence that the MW and M31 satellites are dark matter rich (assuming conventional CDM cosmology). Another possible difference between the TDG discovered in this study and local dwarf satellites is their gas content. Despite several Gyr of evolution, the TDGs around NGC 5557 are still gas-rich. This reflects their origin as tidally expelled condensations made almost entirely of gas and suggests a rather low efficiency at converting gas into stars after the initial collapse and inefficient gas blow-away and stripping mechanisms. Whether the puzzling ability of keeping gas is something specific to the system studied here or an intrinsic characteristics of TDGs born in H I tidal tails remains to be determined.

In any case, the origin of the DoSs remains mysterious: the dwarf galaxy accretion at the heart of the hierarchical cosmological models cannot easily reproduce such narrow distribution of satellites. One possibility to investigate is whether the DoSs are made of objects with an origin similar to TDGs, i.e. born within larger structures, but not strictly speaking within tidal debris produced by major mergers, as those so far considered for the tidal dwarfs. These could be dwarfs originating in the massive clumps observed in distant gas-rich galaxies (e.g. Elmegreen et al. 2007; Bournaud et al. 2007) and then kicked out due to clump-clump interactions or dwarfs born together within gaseous cosmological filaments.

## 5 SUMMARY AND CONCLUSIONS

We have obtained with Gemini-North optical long-slit spectra of a sample of 7 dwarf galaxies in the vicinity of 5 early-type galaxies (ETGs) selected from the ATLAS<sup>3D</sup> survey. Deep optical CFHT/MegaCam images and WSRT radio observations had previously detected around the selected ETGs gaseous and/or stellar streams that made the host galaxies likely old gas-rich mergers, and their dwarf satellites excellent tidal dwarf galaxy (TDGs) candidates. The spectroscopic observations were aimed at measuring the oxygen abundance of the ETG satellites, and investigate any deviation from the mass-metallicity relation that may indicate a tidal origin. We furthermore used the MegaCam images to determine the morphological properties of the dwarfs and their behavior with respect to standard scaling relations. We obtained the following results:

- One dwarf, referred as NGC 5557-E1, located in the vicinity of the massive elliptical, NGC 5557, has a gas-phase metallicity of about solar; its oxygen abundance is 0.6 dex above that typical of regular dwarf galaxies, or conversely its abundance corresponds to that of a galaxy ten times more massive. This dwarf, together with two fainter companion objects, E2 and E3 (for which no spectra could be extracted), lie along an extended, very low surface brightness tidal tail, most likely formed during a major merger that occurred at least 2 Gyr ago. A burst model fitting the spectral energy distribution of NGC 5557-E1 provides an age for the dwarf of about 4 Gyr, consistent with the age estimate of the merger at the origin of NGC 5557. Object E1, plus most likely its companions located in the same tidal structure, in particular the apparently relaxed object E2, would thus be the oldest confirmed tidal dwarf galaxies so far identified.

- Like regular dwarf ellipticals/spheroidals, NGC 5557-E1/E2 are well fitted by exponential light profiles. However, they have an unusually large effective radius, and low central surface brightness for their mass. This may be an intrinsic characteristic of old TDGs. Besides, contrary to typical satellites of massive galaxies, NGC 5557-E1/E2 managed to retain a large gas reservoir despite several Gyr of evolution and interaction with their parent galaxy.

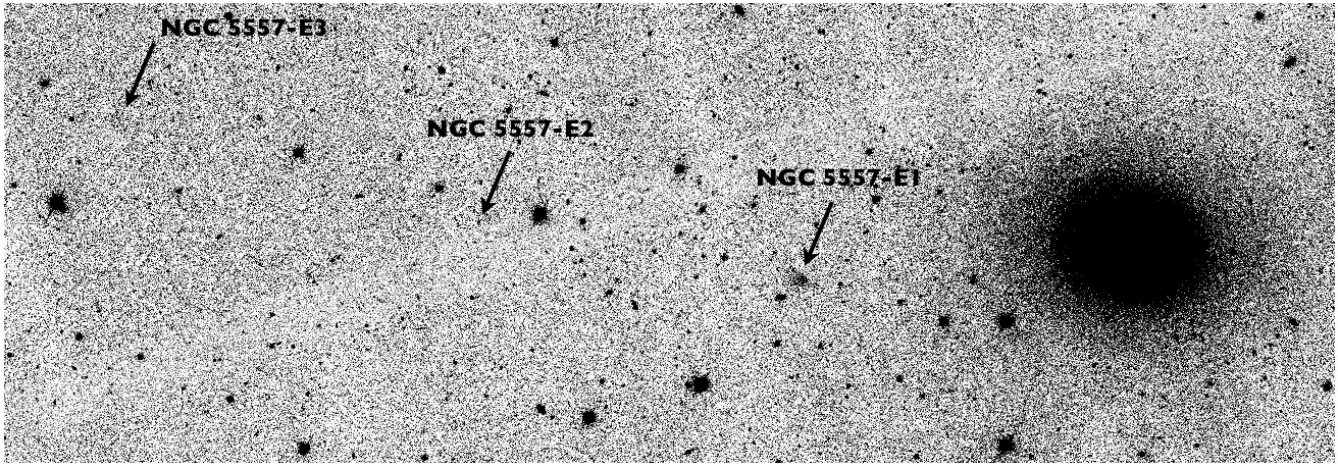


Figure 10. SDSS g-band image of the field around NGC 5557

They may preserve it for several additional Gyr, given their very low current star-formation rate, as measured from the UV and/or  $H_{\alpha}$  luminosity, unless stripping mechanisms become important.

- Among the four other ETG satellites in our survey, three that are more massive than NGC 5557-E1/E2 tend to also have rather low central surface brightness and large effective radius. However unlike the confirmed TDGs, they are not clear outliers of the luminosity-metallicity relation. In fact, the method to identify TDGs using deviations from scaling relations only works well for low-mass objects. Future systematic surveys of tidal dwarfs should thus rather focus on the least massive ones, identified in deep images. They may tell whether the large effective radius found for the old TDGs NGC 5557-E1/E2, but also for young TDGs, is a durable, intrinsic characteristic of a tidal origin. If this is the case, it is then unlikely that the dwarfs in the disk of satellites around our Milky Way and Andromeda are old TDGs made in gas-rich major mergers.

## ACKNOWLEDGMENTS

We first express our gratitude to the anonymous referee for his very careful reading of the paper and for spotting a few inconsistencies in some tables which forced us to check and revise our measurements. This work would not have been possible without the wealth of data acquired as part of the ATLAS<sup>3D</sup> collaboration. We are grateful to all team members. We warmly thank Raphael Gobat for his help with the SED fitting. This paper made use of spectra obtained at the Gemini Observatory, which is operated by the Association of Universities for Research in Astronomy, Inc., under a cooperative agreement with the NSF on behalf of the Gemini partnership: the National Science Foundation (United States), the National Research Council (Canada), CONICYT (Chile), the Australian Research Council (Australia), Ministério da Ciência, Tecnologia e Inovação (Brazil) and Ministerio de Ciencia, Tecnología e Innovación Productiva (Argentina). This study was also partly based on observations obtained with MegaPrime/MegaCam, a joint project of CFHT and CEA/IRFU, at the Canada-France-Hawaii Telescope (CFHT) which is operated by the National Research Council (NRC) of Canada, the Institut National des Science de l'Univers of the Centre National de la Recherche Scientifique (CNRS) of France, and the Univer-

sity of Hawaii. SDSS data were queried from the SDSS archives. Funding for the SDSS and SDSS-II has been provided by the Alfred P. Sloan Foundation, the Participating Institutions, the National Science Foundation, the U.S. Department of Energy, the National Aeronautics and Space Administration, the Japanese Monbukagakusho, the Max Planck Society, and the Higher Education Funding Council for England. The SDSS Web Site is <http://www.sdss.org>. The SDSS is managed by the Astrophysical Research Consortium for the Participating Institutions. The Participating Institutions are the American Museum of Natural History, Astrophysical Institute Potsdam, University of Basel, University of Cambridge, Case Western Reserve University, University of Chicago, Drexel University, Fermilab, the Institute for Advanced Study, the Japan Participation Group, Johns Hopkins University, the Joint Institute for Nuclear Astrophysics, the Kavli Institute for Particle Astrophysics and Cosmology, the Korean Scientist Group, the Chinese Academy of Sciences (LAMOST), Los Alamos National Laboratory, the Max-Planck-Institute for Astronomy (MPIA), the Max-Planck-Institute for Astrophysics (MPA), New Mexico State University, Ohio State University, University of Pittsburgh, University of Portsmouth, Princeton University, the United States Naval Observatory, and the University of Washington. This work is supported by the French Agence Nationale de la Recherche (ANR) Grant Programme Blanc VIRAGE (ANR10-BLANC-0506-01). MC acknowledges support from a Royal Society University Research Fellowship. This work was supported by the rolling grants Astrophysics at Oxford PP/E001114/1 and ST/H002456/1 and visitors grants PPA/V/S/2002/00553, PP/E001564/1 and ST/H504862/1 from the UK Research Councils. RMCD is supported by the Gemini Observatory, which is operated by the Association of Universities for Research in Astronomy, Inc., on behalf of the international Gemini partnership of Argentina, Australia, Brazil, Canada, Chile, the United Kingdom, and the United States of America.

## REFERENCES

- Asplund M., Grevesse N., Sauval A. J., 2005, in Barnes III T. G., Bash F. N., eds, ASP Conf. Ser. 336: Cosmic Abundances as Records of Stellar Evolution and Nucleosynthesis  
 Bell E. F., McIntosh D. H., Katz N., Weinberg M. D., 2003, *ApJS*, 149, 289

- Bellazzini M., Oosterloo T., Fraternali F., Beccari G., 2013, *A&A*, 559, L11
- Belles P.-E., Duc P.-A., Brinks E. e., 2014, *A&A*, submitted
- Bois M., Emsellem E., Bournaud F., Alatalo K., Blitz L., Bureau M., et al. 2011, *MNRAS*, 416, 1654
- Boquien M., Duc P.-A., Galliano F., Braine J., Lisenfeld U., Charmandaris V., Appleton P. N., 2010, *AJ*, 140, 2124
- Bournaud F., Duc P.-A., 2006, *A&A*, 456, 481
- Bournaud F., Duc P.-A., Emsellem E., 2008, *MNRAS*, 389, L8
- Bournaud F., Elmegreen B. G., Elmegreen D. M., 2007, *ApJ*, 670, 237
- Braine J., Duc P.-A., Lisenfeld U., Charmandaris V., Vallejo O., Leon S., Brinks E., 2001, *A&A*, 378, 51
- Brasseur C. M., Martin N. F., Macciò A. V., Rix H.-W., Kang X., 2011, *ApJ*, 743, 179
- Bruzual G., Charlot S., 2003, *MNRAS*, 344, 1000
- Calzetti D., Armus L., Bohlin R. C., Kinney A. L., Koornneef J., Storchi-Bergmann T., 2000, *ApJ*, 533, 682
- Cappellari M., Emsellem E., Krajnović D., McDermid R. M., Scott N., Verdoes Kleijn G. A., Young L. M., 2011, *MNRAS*, 413, 813
- Dabringhausen J., Kroupa P., 2013, *MNRAS*, 429, 1858
- Di Matteo P., Bournaud F., Martig M., Combes F., Melchior A.-L., Semelin B., 2008, *A&A*, 492, 31
- Duc P.-A., 2012, in Papaderos P., Recchi S., Hensler G., eds, *Dwarf Galaxies: Keys to Galaxy Formation and Evolution*. Springer-Verlag Berlin Heidelberg, p. 305
- Duc P.-A., Bournaud F., Masset F., 2004, *A&A*, 427, 803
- Duc P.-A., Braine J., Lisenfeld U., Brinks E., Boquien M., 2007, *A&A*, 475, 187
- Duc P.-A., Cuillandre J.-C., Serra P., Michel-Dansac L., Ferriere E., Alatalo K., Blitz L., Bois M., Bournaud F., 2011, *MNRAS*, 417, 863
- Duc P.-A., Mirabel I. F., 1994, *A&A*, 289, 83
- Duc P.-A., Papaderos P., Balkowski C., Cayatte V., Thuan T. X., van Driel W., 1999, *A&AS*, 136, 539
- Elmegreen D. M., Elmegreen B. G., Ferguson T., Mullan B., 2007, *ApJ*, 663, 734
- Fellhauer M., Kroupa P., 2002, *MNRAS*, 330, 642
- Ferrarese L., Côté P., Cuillandre J.-C., Gwyn S. D. J., Peng E. W., et al. 2012, *ApJS*, 200, 4
- Fleck J.-J., Kuhn J. R., 2003, *ApJ*, 592, 147
- Gavazzi G., Donati A., Cucciati O., Sabatini S., Boselli A., Davies J., Zibetti S., 2005, *A&A*, 430, 411
- Hammer F., Yang Y., Fouquet S., Pawlowski M. S., Kroupa P., Puech M., Flores H., Wang J., 2013, *MNRAS*, 431, 3543
- Hancock M., Smith B. J., Struck C., Giroux M. L., Hurlock S., 2009, *AJ*, 137, 4643
- Hibbard J. E., Mihos J. C., 1995, *AJ*, 110, 140
- Hunsberger S. D., Charlton J. C., Zaritsky D., 1996, *ApJ*, 462, 50
- Hunter D. A., Hunsberger S. D., Roye E. W., 2000, *ApJ*, 542, 137
- Ibata R. A., Lewis G. F., Conn A. R., Irwin M. J., McConnachie A. W., Chapman S. C., Collins M. L., Fardal M., Ferguson A. M. N., Ibata N. G., Mackey A. D., Martin N. F., Navarro J., Rich R. M., Valls-Gabaud D., Widrow L. M., 2013, *Nature*, 493, 62
- Kaviraj S., Darg D., Lintott C., Schawinski K., Silk J., 2012, *MNRAS*, 419, 70
- Kennicutt Jr. R. C., 1998, *ARA&A*, 36, 189
- Kirby E. M., Jerjen H., Ryder S. D., Driver S. P., 2008, *AJ*, 136, 1866
- Krajnović D., Emsellem E., Cappellari M., Alatalo K., Blitz L., et al. 2011, *MNRAS*, 414, 2923
- Libeskind N. I., Knebe A., Hoffman Y., Gottlöber S., Yepes G., Steinmetz M., 2011, *MNRAS*, 411, 1525
- Lynden-Bell D., 1976, *MNRAS*, 174, 695
- Marino R. A., Rosales-Ortega F. F., Sánchez S. F., Gil de Paz A., Vílchez J., et al. 2013, *A&A*, 559, A114
- Mayer L., Governato F., Colpi M., Moore B., Quinn T., Wadsley J., Stadel J., Lake G., 2001, *ApJ*, 559, 754
- Mayer L., Mastroiello C., Wadsley J., Stadel J., Moore B., 2006, *MNRAS*, 369, 1021
- Mendes de Oliveira C., Plana H., Amram P., Balkowski C., Bolte M., 2001, *AJ*, 121, 2524
- Metz M., Kroupa P., 2007, *MNRAS*, 376, 387
- Michel-Dansac L., Martig M., Bournaud F., Emsellem E., Duc P. A., Combes F., 2010, in V. P. Debattista & C. C. Popescu ed., *Hunting for the dark: the hidden side of galaxy formation* Vol. 1240 of American Institute of Physics Conference Series, p. 283
- Miralles-Caballero D., Colina L., Arribas S., 2012, *A&A*, 538, A61
- Misgeld I., Hilker M., 2011, *MNRAS*, 414, 3699
- Misgeld I., Mieske S., Hilker M., 2008, *A&A*, 486, 697
- Neff S. G., Thilker D. A., Seibert M., Gil de Paz A., Bianchi L., et al. 2005, *ApJ*, 619, L91
- Okazaki T., Taniguchi Y., 2000, *ApJ*, 543, 149
- Paudel S., Duc P.-A., Côté P., Cuillandre J.-C., Ferrarese L., Ferriere E., Gwyn S. D. J., 2013, *ApJ*, 767, 133
- Pawlowski M. S., Kroupa P., Angus G., de Boer K. S., Famaey B., Hensler G., 2012, *MNRAS*, 424, 80
- Ploekinger S., Hensler G., Recchi S., Mitchell N., Kroupa P., 2014, *MNRAS*, 437, 3980
- Recchi S., Theis C., Kroupa P., Hensler G., 2007, *A&A*, 470, L5
- Richer M. G., McCall M. L., 1995, *ApJ*, 445, 642
- Serra P., Oosterloo T., Morganti R., et al. 2012, *MNRAS*, 422, 1835
- Sérsic J. L., 1968, *Bulletin of the Astronomical Institutes of Czechoslovakia*, 19, 105
- Smith B. J., Giroux M. L., Struck C., Hancock M., 2010, *AJ*, 139, 1212
- Smith R., Duc P. A., Candlish G. N., Fellhauer M., Sheen Y.-K., Gibson B. K., 2013, *MNRAS*, 436, 839
- Sweet S. M., Drinkwater M. J., Meurer G., Bekki K., Dopita M. A., Kilborn V., Nicholls D. C., 2014, *ApJ*, 782, 35
- Tremonti C. A., Heckman T. M., Kauffmann G., Brinchmann J., Charlot S., White S. D. M., Seibert M., Peng E. W., Schlegel D. J., Uomoto A., Fukugita M., Brinkmann J., 2004, *ApJ*, 613, 898
- van Zee L., Haynes M. P., 2006, *ApJ*, 636, 214
- Weilbacher P. M., Duc P.-A., Fritze-v. Alvensleben U., 2003, *A&A*, 397, 545
- Weilbacher P. M., Duc P.-A., Fritze v. Alvensleben U., Martin P., Fricke K. J., 2000, *A&A*, 358, 819
- Wetzstein M., Naab T., Burkert A., 2007, *MNRAS*, 375, 805